Can. J. Remote Sensing, Vol. 30, No. 1, pp. 17–25, 2004

Observation of chlorophyll fluorescence in west coast waters of Canada using the MODIS satellite sensor

J.F.R. Gower, L. Brown, and G.A. Borstad

Abstract. The first observations of chlorophyll fluorescence from space for the west coast of Canada, using the U.S. moderate resolution imaging spectrometer (MODIS), show that the signals should provide a useful new tool for studying chlorophyll biomass and primary productivity. We compare MODIS fluorescence and sea-viewing wide field-of-view sensor (SeaWiFS) chlorophyll data, using a simple theoretical model of the expected variation of fluorescence emission with variations in chlorophyll concentration. The results show good agreement with the model and appear to allow separation of water masses according to fluorescence yield. As additional MODIS data come available it will be possible to study data for the full range of seasonal conditions. Additional data from the European medium-resolution imaging spectrometer (MERIS) sensor are available from 2002.

Résumé. Les premières observations de la fluorescence chlorophyllienne à partir de l'espace pour la côte ouest du Canada réalisées par le capteur américain MODIS (« moderate resolution imaging spectrometer ») montrent que ces signaux pourraient constituer un outil utile pour l'étude de la biomasse chlorophyllienne et de la productivité primaire. Nous comparons la fluorescence de MODIS et les données de chlorophylle de SeaWiFS utilisant un modèle théorique simple de la variation projetée de l'émission de la fluorescence en fonction de la concentration de chlorophylle. Les résultats montrent une bonne correspondance avec le modèle et semblent permettre la séparation des masses d'eau en fonction du rendement de fluorescence. À mesure que les données MODIS deviendront disponibles, il sera possible d'étudier des données pour toute une gamme de conditions saisonnières. Des données additionnelles du capteur européen MERIS sont disponibles depuis 2002.
[Traduit par la Rédaction]

Introduction

The moderate resolution imaging spectrometer (MODIS) sensor on the U.S. Terra satellite is designed to provide images at optical wavebands suitable for computing chlorophyll concentrations and other properties of phytoplankton. This is the first satellite sensor to make global measurements of solar-stimulated fluorescence. This signal provides an alternative means of measuring chlorophyll concentrations and gives additional information on phytoplankton state and productivity. Problems of varying emission per unit concentration of chlorophyll *a* pigment for different species and under different conditions of growth and stress are yet to be quantified or resolved.

Fluorescence is one of three de-excitation pathways, after the radiation of direct or indirect sunlight is absorbed by phytoplankton, the other two being photosynthesis and heat. The emission is centred at 685 nm, with a Gaussian spectral profile having a width at half maximum of 25 nm (Mobley, 1994). $F(\lambda)$, the emission at a wavelength λ, is therefore

$$F(\lambda) = F \exp\{-4 \ln(2) [(\lambda - 685)/25]^2\} \quad (1)$$

where F is the peak fluorescence radiance (in $W \cdot m^{-2} \cdot sr^{-1} \cdot \mu m^{-1}$). **Figure 1** shows a plot of this Gaussian profile for $F = 1$, with positions and widths of MODIS and medium resolution imaging spectrometer (MERIS) bands. MERIS bands are programmable, but the baseline band set (from which bands are shown here) will be used for most observations. Assuming this spectral profile for fluorescence, the signal drops to half its peak at 672.5 and 697.5 nm and to less than 5% at wavelengths shorter than 650 nm or longer than 720 nm.

The MODIS sensor provides images with a spatial resolution of 1 km in bands centred at 411.3, 442.0, 486.9, 529.6, 546.8, 665.5, 677.6, 746.4, and 866.2 nm; bandwidths are near 15 nm at wavelengths 411.3 and 866.2 nm, 12.0 nm at wavelength 529.6 nm, 11.3 nm at wavelength 676.8 nm, and near 10 nm at all other wavelengths (NASA, 2000). Bands between 442 and 547 nm allow calculation of chlorophyll concentrations by blue to green ratio or other algorithms based on absorption properties of chlorophyll pigments at these wavelengths. Bands at 665.5, 677.6, and 746.4 nm can be used to compute the fluorescence emitted by chlorophyll *a*.

Bands to detect the fluorescence are placed to measure the fluorescence signal and also to define a linear baseline above

Received 7 May 2002. Accepted 23 June 2003.

J.F.R. Gower.[1] Institute of Ocean Sciences, P.O. Box 6000, Sidney, BC V8L 4B2, Canada.

L. Brown and G.A. Borstad. G.A. Borstad Associates Ltd., Sidney, BC V8L 5Y8, Canada.

[1]Corresponding author (e-mail:gowerj@pac.dfo-mpo.gc.ca).

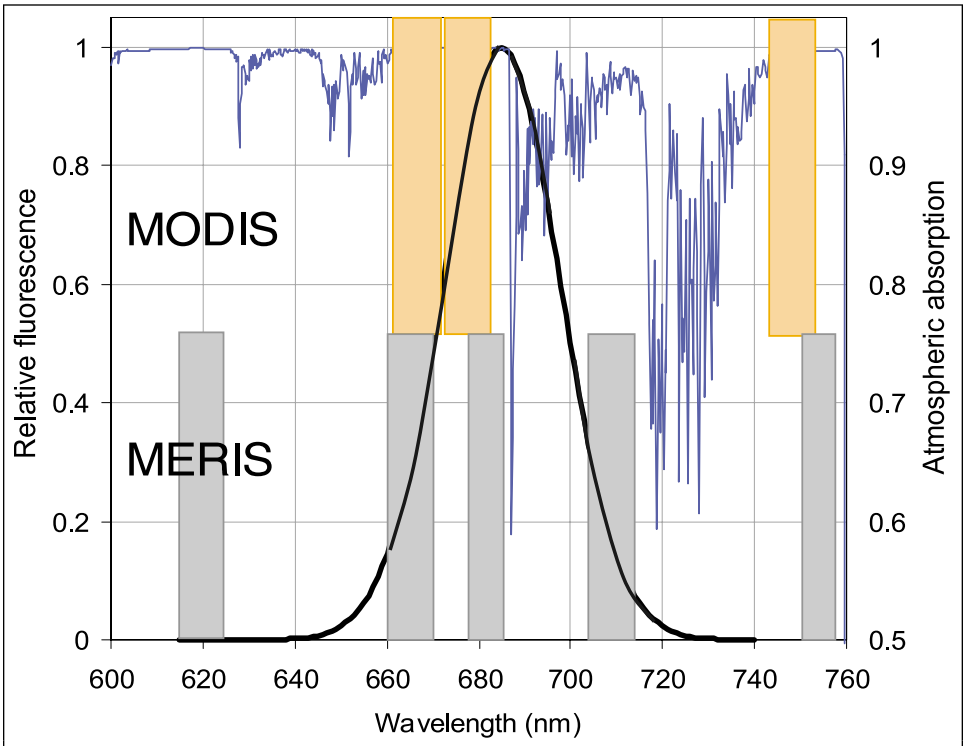

Figure 1. Theoretical phytoplankton fluorescence, showing positions and widths of MODIS and MERIS bands and atmospheric absorption features.

which the signal is measured. For MODIS, the baseline bands are centred at 665.5 and 746.4 nm. As shown in **Figure 1**, the 665.5 nm band will also contain some fluorescence signal. For the aforementioned theoretical band profile, relative signals due to fluorescence are 0.20 for the 665.5 nm band, 0.74 for the 676.8 nm band, and <0.001 for the 746.4 nm band. That is, the 676.8 nm band detects only 74% of the peak radiance of the fluorescence signal. The MODIS bands are defined by filters that do not have the perfectly sharp edges shown in **Figure 1**. The 676.8 nm band therefore had to be placed at this relatively short wavelength to avoid the effects of strong atmospheric absorption due to oxygen at wavelengths longer than 686.7 nm, also plotted in **Figure 1**. The reference band at 665.5 nm, which would ideally be outside the fluorescence range, should in fact detect 20% of the peak signal. This band was placed at this relatively long wavelength partly to avoid absorption bands, and partly to minimize the wavelength interval between the fluorescence, and one of the reference wavelengths. This improves the rejection of broadband interfering signals, such as atmospheric radiance.

The linear baseline fluorescence algorithm computes a fluorescence line height (FLH) radiance from the radiances $L(\lambda_1)$, $L(\lambda_2)$, and $L(\lambda_3)$ (in $W \cdot m^{-2} \cdot sr^{-1} \cdot \mu m^{-1}$), where λ_2 is the "fluorescence" band, as

$$FLH = L(\lambda_2) - kL(\lambda_1) - (1 - k)L(\lambda_3) \quad (2)$$

where $k = (746.4 - 676.8)/(746.4 - 665.5) = 0.860$ for MODIS bands. The high value of k for MODIS means that the baseline radiance signal to be subtracted at 676.8 nm is mostly defined by the 665.5 nm band. Since this responds to 20% of the peak signal, and the measured fluorescence is only 74% of the peak, the formula shows that MODIS will be responding to only 57% of the actual fluorescence signal. We call this 0.57 the FLH reduction factor for MODIS. The FLH reduction factor for MERIS is 0.78.

The computed FLH will ideally use water-leaving radiance values in each of the three bands. However, derivation of these radiances implies accurate atmospheric correction. FLH can also be computed from the top-of-atmosphere radiances, which are the values initially computed from a satellite sensor (level 1 data) using instrument calibration information. In this case, an offset in fluorescence must be expected because of the effect on Equation (2) of the nonlinear change of atmospheric radiance with a change in wavelength. Also, absorption by the atmosphere is typically about 10% at wavelengths near 685 nm.

Expected fluorescence signal level in MODIS data

The amount of emitted signal is expected to vary with variation in the chlorophyll *a* pigment concentration, but is also expected to be affected by photoinhibition, phytoplankton species, and physiological state (Kiefer, 1973; Falkowski and Kiefer, 1985). We assume average illumination, species, and state conditions for a first estimate, though it should be noted that all cloud-free satellite images are taken under conditions of full sunlight, given the "near local noon" orbit of the TERRA

satellite. A considerable amount of photoinhibition is therefore to be expected.

Peak fluorescence radiance F in Equation (1) varies with variation in the chlorophyll *a* pigment concentration, C. At low values of C (<0.01 mg·m^{-3}) the fluorescence signal is limited by the absorption of water and increases linearly with an increase in C. The expected fluorescence emission (in W·m^{-2}·sr^{-1}·μm^{-1}) for zenith sun and low atmospheric absorption, at a concentration C (in mg·m^{-3}), based on an average of reported measurements (Gower, 1999), is

$$F(C) = 0.15C \quad (3)$$

At higher values of C, an increasing fraction of the stimulating and emitted fluorescence signals is absorbed by the phytoplankton itself, so an increase in phytoplankton concentration does not lead to a proportional increase in signal. Both the stimulating short-wave solar irradiance and the emitted fluorescence at 685 nm are absorbed. By analogy with the findings of Morel and Prieur (1977) and others, water-leaving radiance decreases as $1/a$, where a is the total absorption. Equation (3) then becomes

$$F(C) = 0.15C\,[a_w/(a_w + a_cC)] \quad (4)$$

where a_w and a_c are the total of the absorptions (m^{-1}) affecting the stimulating and emitted fluorescence radiation because of water and chlorophyll pigments, respectively. As a first approximation we take values for absorption of stimulating radiation (over the wavelength range 400–500 nm) by water and by a concentration C (mg·m^{-3}) of chlorophyll pigments as 0.01 and $0.05C$ per metre, respectively, and of emitted fluorescence radiation (at 685 nm) by water and chlorophyll pigments as 0.486 and $0.05C$ per metre, respectively. Then a_w is 0.50 per metre, and a_c is $0.10C$ per metre. The expected fluorescence signal for a chlorophyll concentration C is then

$$F(C) = 0.15C/(1 + 0.20C) \quad (5)$$

Figure 2 shows a plot of this relation. The increase of F with an increase in C is close to linear up to C = 0.5 mg·m^{-3}, but the rate of increase drops by a factor of 2 at C = 2 and by a factor of 10 at C = 10 mg·m^{-3}. In a detailed study of solar-stimulated chlorophyll fluorescence, Babin et al. (1996) present a computed relation of F versus C that includes the average variation of fluorescence properties of natural populations with C. Their calculation is for a "moderate" PAR value, equivalent to about half the value for a zenith sun. When this difference is removed, the two curves are in close agreement (**Figure 2**).

As noted earlier in the paper, fluorescence is ideally computed from atmospherically corrected water-leaving radiances (level 2 data). As shown later in the paper, however, there may be problems in making these corrections, and the simple alternative exists of computing fluorescence from level 1 (top-of-atmosphere) radiances, relying on the linear baseline fluorescence calculation to reduce the contribution of the (relatively high) atmospheric radiance to an acceptably small error. Level 1 fluorescence will be low by about 10% because of the diffuse attenuation of the atmosphere near 685 nm.

Also, the atmospheric radiance must be expected to introduce an offset, depending on the spectral properties of this radiance near 685 nm and the wavelengths used in the calculation. The magnitude and spectral properties of the radiance are expected to vary with aerosol loading of the atmosphere. For a clear atmosphere in which Rayleigh scattering is dominant, the expected offset for a solar elevation of 90° and the MODIS bandset is –0.165 W·m^{-2}·sr^{-1}·μm^{-1}. For the MERIS bandset, the offset is –0.063 W·m^{-2}·sr^{-1}·μm^{-1}, a smaller value, since the three bands used are closer together. In both cases the offsets are relatively small and should vary smoothly over scenes about 1000 km across. Offsets are due to almost equal contributions from curvature of the spectra of the sun and of the Rayleigh scattering.

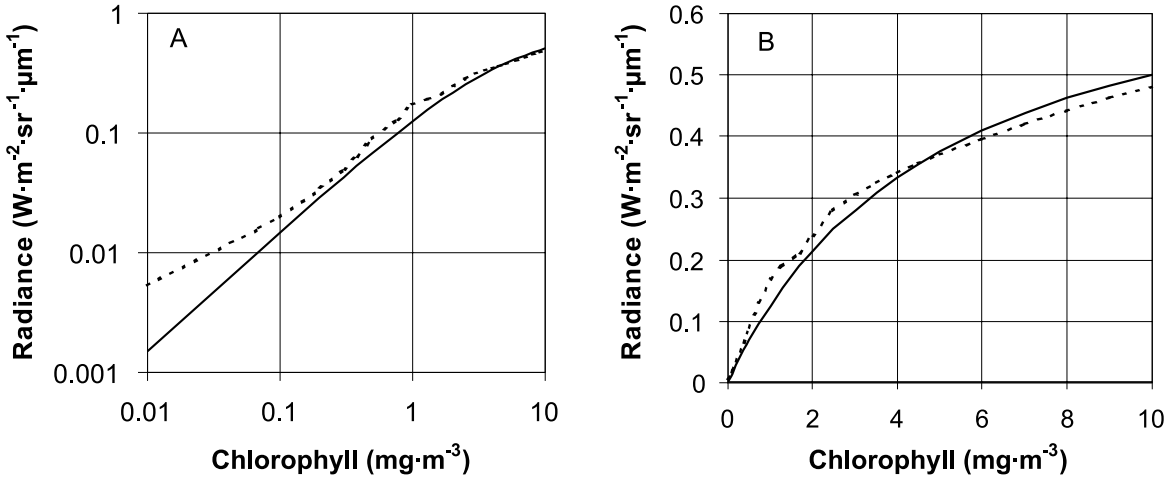

Figure 2. Fluorescence curves, predicted according to Equation (5) (solid line) and Babin et al. (1996) (broken line) and plotted on logarithmic (A) and linear (B) scales. The Babin et al. curve is scaled up by a factor of 2 to adjust for high-sun conditions.

Chlorophyll fluorescence observed with MODIS

Figure 3 shows data from 22 September 2000 for the Vancouver Island area. Here, we expect oceanic conditions offshore, and surface outflow of fresh water from the Fraser and other rivers creates an estuarine environment in coastal waters sheltered by Vancouver Island. Outflow south and north of the island spreads low-salinity water containing significant levels of dissolved organic material (case 2 optical conditions; Morel and Prieur, 1977) onto the adjacent continental shelf.

Each image shows a single parameter, displayed with a pseudocolour scale increasing from blue to red. Images are navigated using in-house software that uses the position information embedded in the National Aeronautics and Atmospheric Administration (NASA) hierarchical data format (HDF) data files and takes account of the multiple-sensor, "whisk-broom" scanning. **Figure 3A** shows the NASA fluorescence product in the early level 2 data (NASA, 2000). The resolution of this product has been degraded to 5 km by NASA to improve the signal-to-noise ratio and suppress striping. Unfortunately, this also suppresses finer scale features. **Figure 3B** shows the result of computing the fluorescence signal from the 665.5, 676.8, and 746.4 nm radiances in the level 1 product. This gives improved spatial resolution compared with that of the degraded level 2 product, but striping masks some of the more subtle features. **Figure 3C** shows the result of empirical destriping, using a reference area of relatively clear water.

Figure 3C shows improved spatial resolution compared with that of the NASA level 2 product available in 2002. The larger scale features in the two products are very similar, but the smoothing in the NASA product has blurred many of the smaller scale features. Also, significant low-fluorescence (dark blue) features appear, for example near the coast of Washington State and in Juan de Fuca Strait, which are not present in **Figure 3A**. To investigate the FLH images further, including

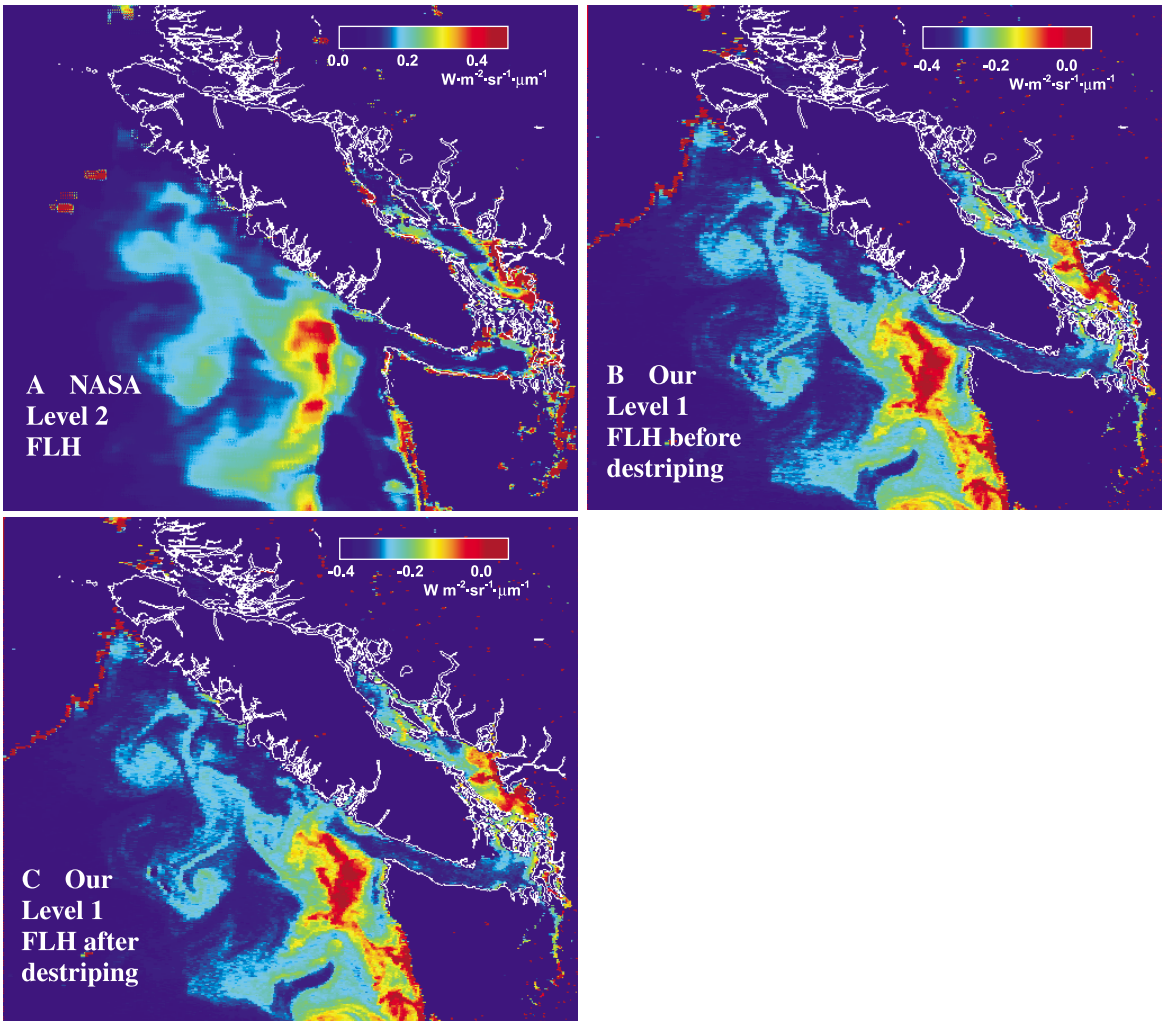

Figure 3. MODIS images for 1855 UTC (about 1100 hours local solar time) on 22 September 2000 for the Vancouver Island area. (A) NASA level 2 fluorescence product. (B) Fluorescence computed from level 1 before destriping. (C) Fluorescence in (B) after destriping.

these features, we now look at the individual bands of MODIS data used in the derivation of the fluorescence product.

The level 1 fluorescence image is produced from top-of-atmosphere radiance images at 665.5, 676.8, and 746.4 nm, which are shown in **Figures 4A**, **4B**, and **4C**, respectively. In each case the radiance values in these images are dominated by the atmospheric signal, which has a strong gradient across the scene, masking any water features.

Figures 4D–4F show the result of "flattening" or "detrending" by removing a mean gradient across the images (second-order polynomial in pixel number). The water-leaving radiance features in the 665.5 and 676.8 nm bands now match many of the features in the fluorescence image in **Figure 3C**. In contrast, the 746.4 nm band shows no water features off the coast of Vancouver Island, though the core of the Fraser River plume is visible. This is as expected from **Figure 1** if a significant fraction of water-leaving radiance in the 665.5 nm and 676.8 nm bands is from chlorophyll fluorescence. In fact, however, a water-leaving radiance signal must be expected over a wide range of wavelengths owing to the optical back-scattering that accompanies elevated phytoplankton densities. This signal could also be significant at 665.5 and 676.8 nm but would be much reduced at 746.4 nm, where water absorption is higher (Pope and Fry, 1997).

The 746.4 nm band shows several areas that can be interpreted as having high atmospheric radiance, including some small cloud patches and larger areas that may be due to variation of sun glint across the image. These same areas appear, more or less brightly, in **Figures 4D** and **4E**, which also show features due to changes in water-leaving radiance. **Figure 3C** is computed from the data in **Figures 4A**–**4C** using the FLH relation (Equation (2)), whose result is relatively insensitive to the gradients in atmospheric radiance shown in those figures. The advantage of this insensitivity is also demonstrated by the fact that in **Figure 3C** the size of the area affected by clouds near the Brooks Peninsula (top left of the images) is significantly reduced compared with that in **Figures 4D**–**4F**.

The features in **Figures 4D** and **4E** are similar to those in **Figure 3C**, with no sign of features that would explain the low-fluorescence area off the west coast of Washington State in **Figure 3A**. NASA acknowledges masking problems with the level 2 fluorescence data, which probably explains these features.

Discussion of the observed fluorescence signal

We now compare the MODIS fluorescence data with chlorophyll data deduced from satellite imagery using the standard blue to green ratio (OC4 algorithm; O'Reilly et al., 1998). Data from MODIS itself would have the advantage of being exactly coincident in time; however, the level 2 ocean-colour products downloaded from NASA for 22 September lacked valid chlorophyll data at the time of this work in mid-2002.

Figure 5 shows the sea-viewing wide field-of-view sensor (SeaWiFS) chlorophyll image for this day at 2100 UTC (coordinated universal time), about 2 h later than MODIS. The same water features are visible. The cloud off Brooks Peninsula has moved significantly to the southeast, with the cloud edge moving about 80 km in the 2 h. Surface winds measured by the coastal meteorological buoys show relatively light, variable winds at the surface (<3 m·s^{-1}), but the upper level winds must have been near 10 m·s^{-1} to explain this movement. Close inspection shows that some water features have also moved appreciably (by 2–3 pixels) between the two scenes, implying water advection speeds of about 0.3 m·s^{-1}.

In **Figure 6** we look for a relation between fluorescence and chlorophyll concentration of the form given by Equation (5) and shown in **Figure 2**. **Figure 6** shows a scatter diagram computed from pixels having valid data in the images shown in **Figures 3C** and **5**. The relation is apparent in the data and is fitted by Equation (5) after a shift of 0.46 W·m^{-2}·sr^{-1}·μm^{-1} of the MODIS points, which could be explained by the effect of atmospheric radiance on level 1 data. This shift is larger than the expected value given earlier in the paper of 0.165 W·m^{-2}·sr^{-1}·μm^{-1} for a Rayleigh-only atmosphere. It is of the expected sign, and the greater magnitude may be explained by the presence of aerosols and (or) by the fact that the Vancouver Island area is near the edge of the MODIS swath on this day. An adjustment of 0.92 has been made to the vertical scale to improve the fit. It was noted previously that the expected adjustment of Equation (5) would be by a factor 0.57 to take account of the reduced sensitivity of MODIS to fluorescence, owing to placement of the instrument's spectral bands. Effectively, we have adjusted Equation (5) by a factor 1.6 in fitting the scatter plot. This fit means that we are seeing 1.6 times the fluorescence signal predicted by Equation (5) and the MODIS FLH reduction factor.

The scatter of points about a mean relation will be partly due to errors in estimating either the fluorescence signal or the chlorophyll concentration. Slight additional scatter will be caused by the movement of water features in the 2 h between the MODIS and the SeaWiFS data. Significant scatter is expected from the variation of fluorescence yield with physiological state of the phytoplankton. This is an important variable whose measurement would allow satellite imagery to address new problems in primary production in marine and inland waters.

Chlorophyll fluorescence deficit

Figure 7 shows the result of mapping the fraction by which points fall above or below the relation in **Figure 6**. The points falling below the curve in **Figure 7** are coloured in the "warmer colours", yellow and red, making this a "fluorescence-deficit" image. The factor shown is (predicted – observed)/predicted. This is high in the area near the coast where the deficit is about 0.5, that is, fluorescence is less by this factor than that implied

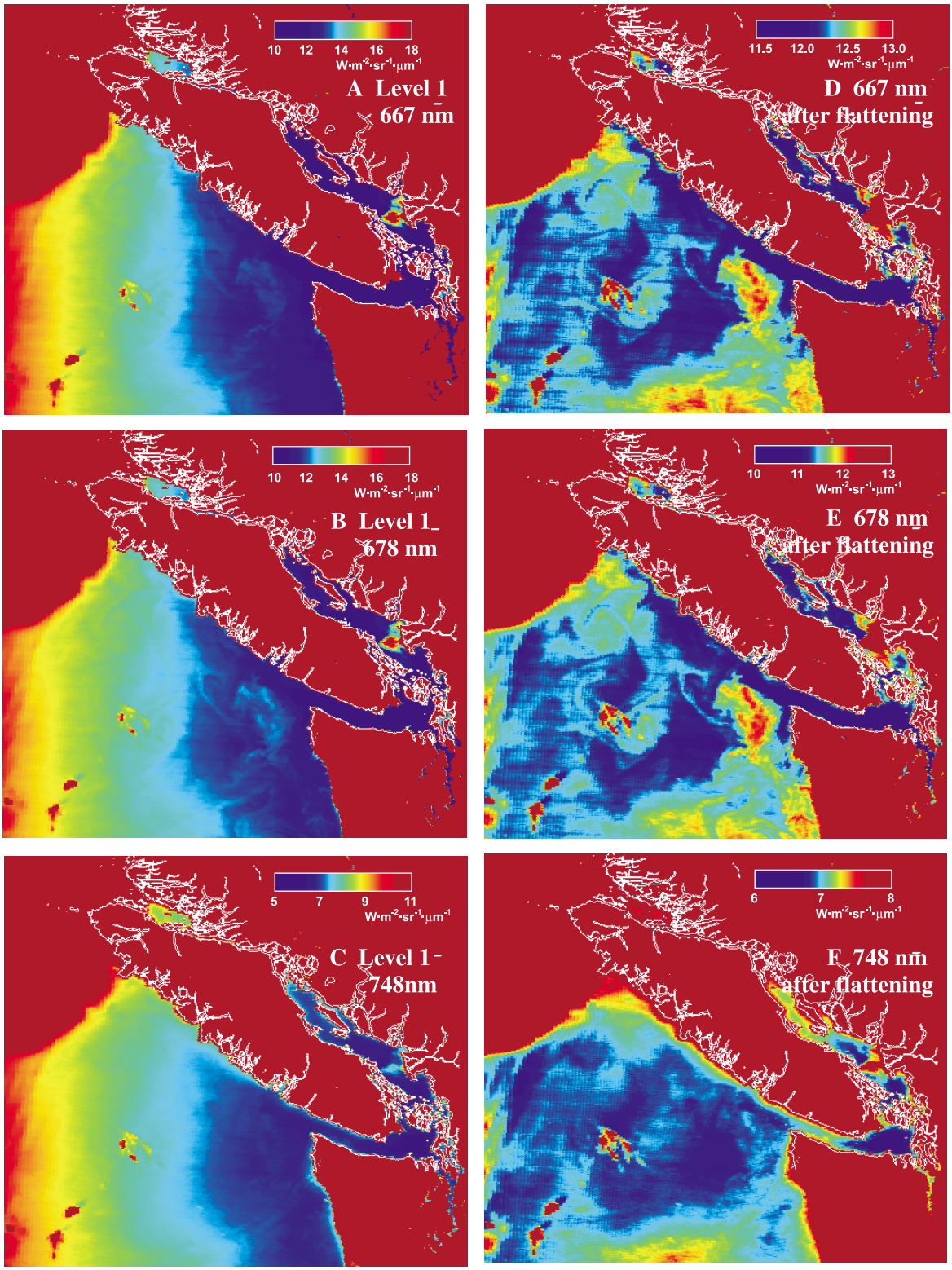

Figure 4. The individual MODIS bands used for deriving the FLH product in **Figure 3** before and after flattening.

by the fitted curve in **Figure 6**. Apparent filaments of high- and low-deficit water in the image correspond to movement of features between the two images.

The area near the coast, shown as "high deficit" in **Figure 7**, is the region of the buoyancy-driven Vancouver Island Coastal Current, where relatively fresh surface water flows alongshore from the mouth of Juan de Fuca Strait to the northwest past the Brooks Peninsula. This water mass is different in many ways from those farther offshore, or in the upwelling area off Juan de Fuca Strait and Washington State. Besides having a shallower,

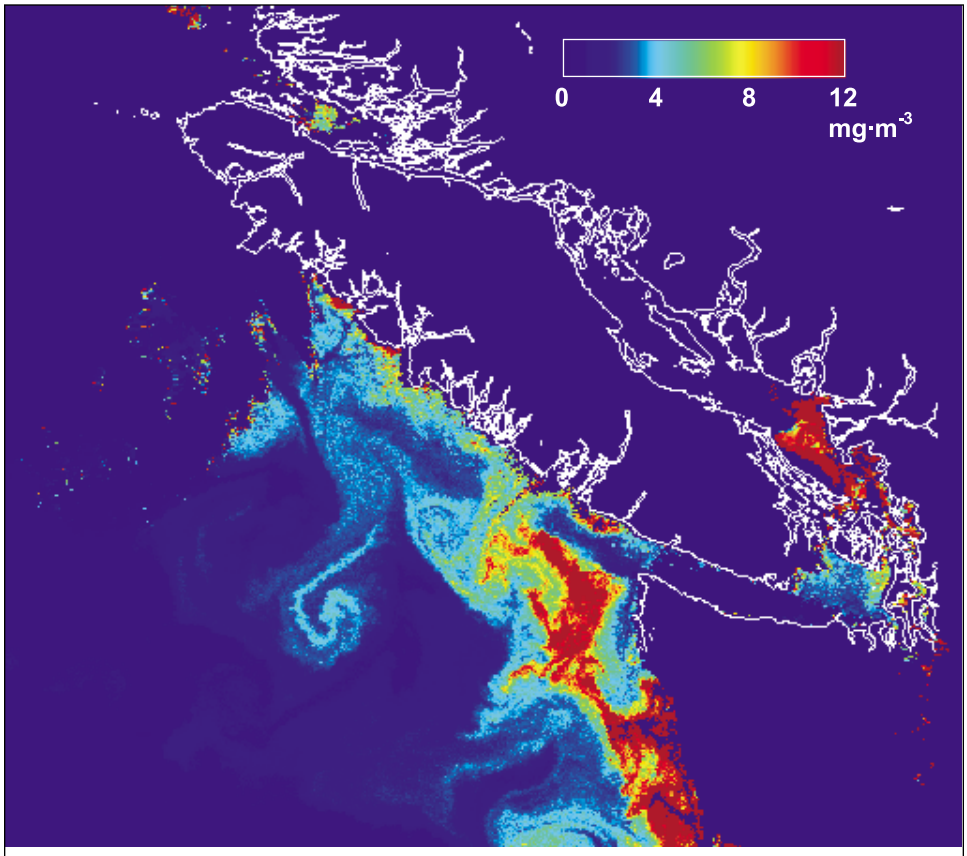

Figure 5. SeaWiFS level 2 chlorophyll product at 2100 UTC on 22 September 2000 for the same area as that shown in **Figures 3** and **4**.

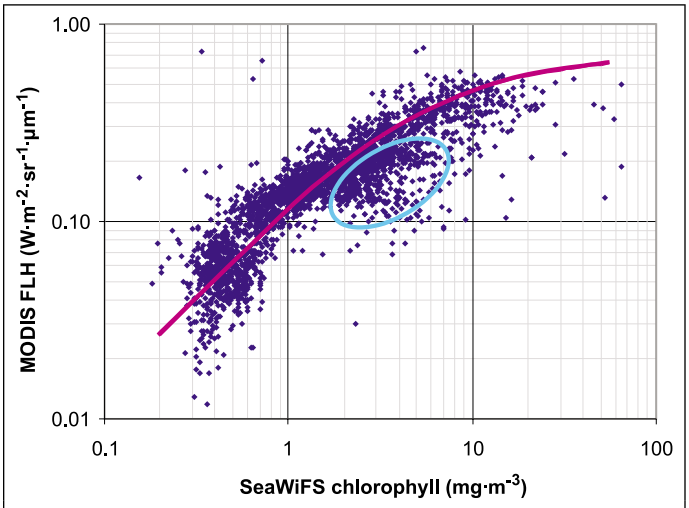

Figure 6. Scatter diagram of SeaWiFS chlorophyll values from **Figure 5** versus MODIS fluorescence from **Figure 3C**, shifted vertically +0.48 $W \cdot^{-2} \cdot sr^{-1} \mu m^{-1}$. The curve is Equation (5), scaled by 0.9 for best fit to the scatter plot. Most of the circled points with the largest fluorescence deficit are located in the Vancouver Island Coastal Current (shown in red in **Figure 7**).

more stratified surface layer, the surface water contains elevated levels of dissolved organic material, whose absorption (of the exciting radiation) would be expected to suppress fluorescence. Fluorescence is an energy-dissipation process, and low fluorescence may also be an indication of rapid phytoplankton growth in which energy is used for photosynthesis rather than emitted as fluorescence. Further investigation of such deficit images is needed.

Also, caution is required in interpreting **Figure 7**, since there is a problem in SeaWiFS level 2 data for the Vancouver Island area, which manifests itself as negative radiances at 412 nm. Clearly such values are unrealistic and indicate an error, either in calibration or in the atmospheric correction. Improved chlorophyll data in case 2 waters should eventually be available from both SeaWiFS and MODIS. This problem is a subject of active research by NASA.

Assuming the chlorophyll data to be accurate, we expect to be able to fit some data in most MODIS images with a curve of the form of Equation (5), using a single radiance offset owing to use of level 1 data and a scaling factor to account for a mean value of solar illumination and fluorescence deficit. Other points will be expected to lie below or above this curve, where deficit values change. In **Figures 6** and **7** we have looked at relative variations in fluorescence deficit about a mean value that appears to be defined predominantly by offshore data. In future it should be possible to interpret the changes in fluorescence deficit by date and area to learn more about their relation to primary production.

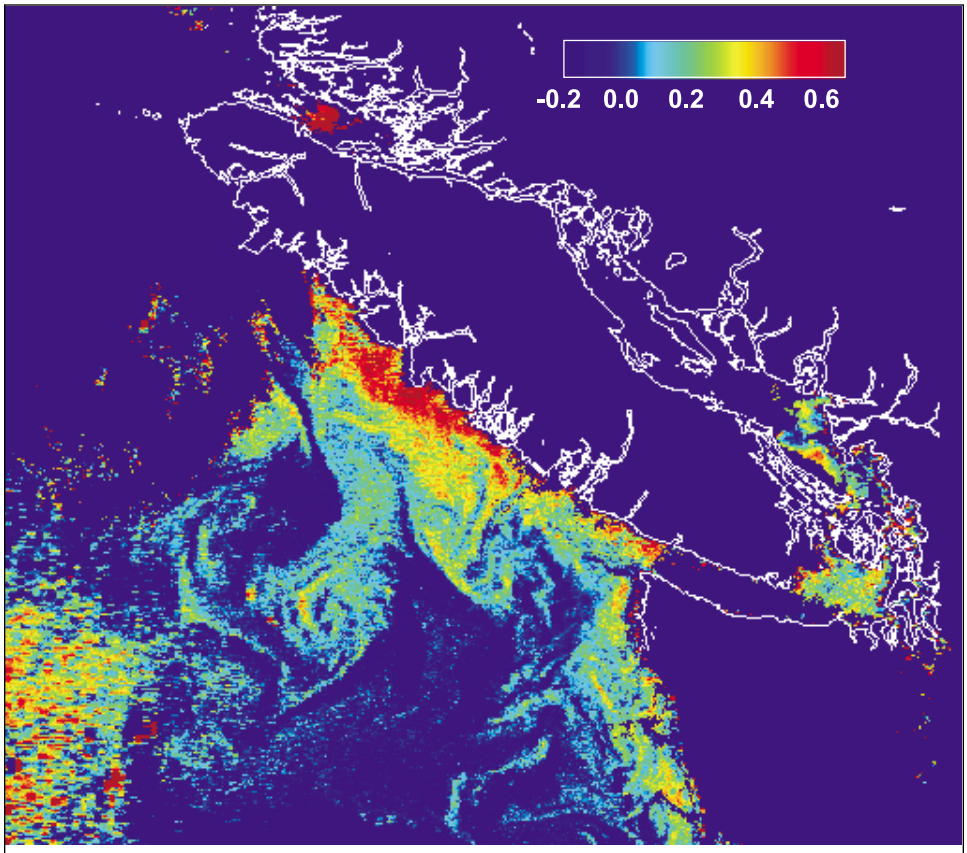

Figure 7. Fluorescence-deficit image, showing the fraction by which the observed fluorescence is less than the expected value represented by the Equation (5) curve.

Conclusions

The MODIS fluorescence data show features in Canadian west coast waters that correspond to chlorophyll as observed by the blue-to-green algorithm method on SeaWiFS. The fluorescence gives added information for phytoplankton mapping and should increase the accuracy of user products. The fluorescence-deficit images show features related to other water mass differences, suggesting further uses for the data that need to be investigated. As with any new technique, the first results shown here suggest possibilities for product improvement, open new questions, and suggest future lines of work. The fluorescence deficit, or the related fluorescence yield, is an extremely important variable whose measurement will allow satellite imagery to address new problems related to primary production in marine and inland waters.

We note that more recent MODIS level 2 data from NASA include unsmoothed fluorescence products, which, as we show, should make the data significantly more useful, especially in coastal areas where finer scale features are expected.

Acknowledgements

This work was funded by the Canadian Space Agency under the Earth Observation Applications Development Program (EOADP), G.A. Borstad Associates Ltd., and Fisheries and Oceans Canada. We are grateful for corrections and useful comments from two anonymous referees.

References

Babin, M., Morel, A., and Gentili, B. 1996. Remote sensing of sea surface sun-induced chlorophyll fluorescence: consequences of natural variations in the optical characteristics of phytoplankton and the quantum yield of chlorophyll *a* fluorescence. *International Journal of Remote Sensing*, Vol. 17, pp. 2417–2448.

Falkowski, P.G., and Kiefer, D.A. 1985. Chlorophyll *a* fluorescence in phytoplankton, relationship to photosynthesis and biomass. *Journal of Plankton Research*, Vol. 7, pp. 715–731.

Gower, J.F.R. 1999. Study of fluorescence-based chlorophyll *a* concentration algorithms for case 1 and case 2 waters. European Space Agency (ESA), European Space Research and Technology Centre (ESTEC), Contract 12295/97/NL/RE.

Kiefer, D.A. 1973. Fluorescence properties of natural phytoplankton populations. *Marine Biology*, Vol. 22, pp. 263–269.

Mobley, C.D. 1994. *Light and water. Radiative transfer in natural waters*. Academic Press, San Diego, Calif. 592 pp.

Morel, A., and Prieur, L. 1977. Analysis of variations in ocean colour. *Limnology and Oceanography*, Vol. 22, pp. 709–722.

NASA. 2000. *EOS data products handbook. Volume 2*. National Aeronautics and Space Administration (NASA), Goddard Space Fight Center, Greenbelt, Md. p. 30.

O'Reilly, J.E., Maritorena, S., Mitchell, B.G., Siegel, D.A., Carder, K.L., Garver, S.A., Kahru, M., and McClain, C. 1998. Ocean color chlorophyll algorithms for SeaWiFS. *Journal of Geophysical Research-Oceans*, Vol. 103, No. C11, pp. 24 937 – 24 953.

Pope, R.M., and Fry, E.S. 1997. Absorption spectrum (370–700 nm) of pure water. II. Integrating cavity measurements. *Applied Optics*, Vol. 36, pp. 8710–8723.